Cavitation-enhanced delivery of insulin in agar and porcine models of human skin

Cavitation-enhanced delivery of insulin in agar and porcine models of human skin

Helga Feiszthuber[1,2]**, Sunali Bhatnagar**[1]**, Miklós Gyöngy**[2] **and Constantin-C Coussios**[1]

[1] Institute of Biomedical Engineering, Department of Engineering Science, University of Oxford, Oxford, UK
[2] Faculty of Information Technology and Bionics, Pázmány Péter Catholic University, Budapest, Hungary

E-mail: feihe@digitus.itk.ppke.hu

CrossMark

Abstract

Ultrasound-assisted transdermal insulin delivery offers a less painful and less invasive alternative to subcutaneous insulin injections. However, ultrasound-based drug delivery, otherwise known as sonophoresis, is a highly variable phenomenon, in part dependent on cavitation. The aim of the current work is to investigate the role of cavitation in transdermal insulin delivery. Fluorescently stained, soluble Actrapid insulin was placed on the surface of human skin-mimicking materials subjected to 265 kHz, 10% duty cycle focused ultrasound. A confocally and coaxially aligned 5 MHz broadband ultrasound transducer was used to detect cavitation. Two different skin models were used. The first model, 3% agar hydrogel, was insonated with a range of pressures (0.25–1.40 MPa peak rarefactional focal pressure—PRFP), with and without cavitation nuclei embedded within the agar at a concentration of 0.05% w/v. The second, porcine skin was insonated at 1.00 and 1.40 MPa PRFP. In both models, fluorescence measurements were used to determine penetration depth and concentration of delivered insulin. Results show that in agar gel, both insulin penetration depth and concentration only increased significantly in the presence of inertial cavitation, with up to a 40% enhancement. In porcine skin the amount of fluorescent insulin was higher in the epidermis of those samples that were exposed to ultrasound compared to the control samples, but there was no significant increase in penetration distance. The results underline the importance of instigating and monitoring inertial cavitation during transdermal insulin delivery.

1. Introduction

Transdermal insulin delivery offers an alternative to conventional insulin delivery methods such as pens and insulin pumps by reducing pain and the chance of infection (Mitragotri *et al* 1995, Khafagy *et al* 2007). For transdermal delivery to be effective, the drug needs to penetrate the natural barriers of the skin. The stratum corneum, the outermost layer of the skin is the biggest barrier inhibiting the penetration of insulin through the skin (Boucaud *et al* 2000, Mitragotri *et al* 2000, Al-Bataineh *et al* 2011, Saroha *et al* 2011); however, recent studies have shown that the full epidermis, not just the stratum corneum is responsible for the low permeability of skin (Andrews *et al* 2013). This finding is important for drugs like insulin that need to reach systemic circulation to perform their function.

The last two decades have seen an exponential increase in the study of ultrasound for enhancing the transdermal transport of a variety of drugs and vaccines, otherwise known as sonophoresis (Levy and kost 1989, Mitragotri *et al* 1996, Boucaud *et al* 2000, Tezel *et al* 2001, Terahara *et al* 2002, Smith *et al* 2003, Prausnitz *et al* 2004, Ogura *et al* 2008, Ueda *et al* 2009, Al-Bataineh *et al* 2011, Kalluri and Banga 2011). The most studied drug is insulin, a 5.6 kDa protein, which is crucial for the wellbeing of type one diabetes mellitus patients. Although low-frequency ultrasound (20–100 kHz) has been shown to be an effective means of transdermal drug delivery (Boucaud *et al* 2000, Prausnitz *et al* 2004, Ogura *et al* 2008, Polat *et al* 2011), in recent years there has been a shift towards middle (100–200 kHz) (Al-Bataineh *et al* 2011) and high (1–3 MHz) frequencies (Mitragotri *et al* 1995, Pitt *et al* 2004). In addition to ultrasound exposure parameters such as frequency and intensity, it is also important to distinguish between ultrasound waves being applied prior to placement of the drug carrier on the skin (*pretreatment sonophoresis*) or after placement (*simultaneous sonophoresis*) (Ogura *et al* 2008, Polat *et al* 2011).

One difficulty with transdermal drug delivery compared with hypodermic needle injection is the uncertainty in delivered dose. This issue is especially important in insulin delivery (Pearson 2010), where international organization for standardizations (ISO) standards require that dose accuracy be within 10% at 10 insulin units (IU) and 5% at 30 IU (Händel *et al* 2008). The measurement of electrical impedance has been shown to be a viable method of monitoring tissue permeability (Mitragotri *et al* 2000, Tezel *et al* 2001, Terahara *et al* 2002), though such measurements are not able to return accurate values of delivered dose. One possible strategy in reducing dose uncertainty is relying on a phenomenon that enables delivery of over 90% of insulin. Cavitation has been shown to be one of the main phenomena involved in sonophoresis, (Prausnitz *et al* 2004) and a number of studies have found correlations between the amount of acoustic cavitation and the delivery achieved. However, these studies have not attempted to quantitatively determine the relationship between the distribution and concentration of ultrasound-enhanced delivery of insulin or any other drug candidate and cavitation activity present during delivery. The current work therefore explores the relationship between acoustic cavitation emissions and final distributions of self-stained fluorescent Actrapid insulin in two tissue-mimicking materials, agar gel and porcine skin.

Though the effects of cavitation in drug delivery have been previously studied, the work serves to better quantify distribution as a function of cavitation activity to better our physical understanding of this phenomenon (Mitragotri *et al* 2000, Tang *et al* 2002, Chen *et al* 2003,

Frenkel 2008, Ueda *et al* 2009, Rifai *et al* 2010, Arvantis *et al* 2011, Mo *et al* 2012, Lai *et al* 2013). In a recent study (Bhatnagar *et al* 2014), inertial cavitation was identified as the dominant mechanism for ultrasound-mediated transport of molecules in agar gels, having a considerably greater impact than either acoustic radiation force or small levels of heating (<2°C). In the present work, the applicability of cavitation-mediated transport to enhancing the delivery of insulin is investigated, through quantification of the level of cavitation activity over a range of ultrasound exposure regimes in agar and porcine skin.

2. Materials and methods

2.1. Overview

The current sub-section gives an overview of the general experimental setup, as shown schematically in figure 1. A high intensity focused ultrasound (HIFU) transducer insonated a sample containing a donor layer with fluorescently stained insulin (see section 2.2) and an acceptor layer containing either agar gel or porcine skin (described in sections 2.3, 2.4, respectively). The insonation happened at various pressures; the employed pressures as well as other settings are detailed in section 2.5. Broadband emissions created by inertial cavitation events were captured by a broadband transducer called a passive cavitation detector, as described in section 2.6. These recordings were then compared with insulin fluorescence measurements that described the spatial distribution of delivered insulin concentration, as detailed in section 2.7. The entire experimental setup was placed in a water tank with deionized, filtered water at room temperature and fitted with a 3D micropositioning system to aid alignment.

2.2. Sample preparation—fluorescently-stained insulin

Actrapid insulin is a neutral, fast acting crystalline insulin. It is the only insulin on the market that is a clear solution, all others being suspensions. This quality makes it ideal for transdermal delivery as well as fluorescent staining. Actrapid insulin (Actrapid Vial 100 IU ml^{-1} solution for injection, Novo Nordisk Ltd, Denmark) was stained with 5-Carboxyflurescein N-succinimidyl ester (CFSE) (Sigma Aldrich, UK) in a ratio of 5 CFSE molecules to 1 insulin molecule for optimal fluorescent visualization. 5 mg CFSE was dissolved in 1 mL dimethylsulfoxide (DMSO) (Sigma-Aldrich, UK), while 1600 μl insulin was dissolved in 8.8 ml phosphate buffered saline (PBS) (Sigma-Aldrich, UK). The two solutions were mixed and shaken for 1 h before filtering with a 3 kDa filter (Amicon Ultra 0.5 ml centrifugal filter, EMD Millipore, MA, USA) to increase insulin concentration and filter out unbound CFSE. The solution was centrifuged up to 8–10 times, each time for a duration of 10 min at a speed of 14 000 rpm, washing with PBS until the liquid in the upper filter compartments turned clear.

Molecular size was determined using Dynamic Light Scattering (DLS) (Zetasizer Nano ZS, laser wavelength 633 nm; Malvern Instruments, UK) before and after staining, in order to rule out the formation of aggregates. The stained insulin molecules had a diameter of 5–7 nm, which was similar to the 5–6 nm diameter of the pure unstained insulin molecules. The final concentration of stained insulin solution was determined using UV/Vis absorbance measurements (FLUOStar Omega, BMG Labtech, Germany), and ranged from 3.72 to 4.72 mg ml^{-1}.

2.3. Sample preparation—agar hydrogel

The agar sample consisted of a donor and an acceptor layer, housed in a cylindrical Perspex holder described in an earlier publication (Bhatnagar *et al* 2014). Briefly, the inner dimensions
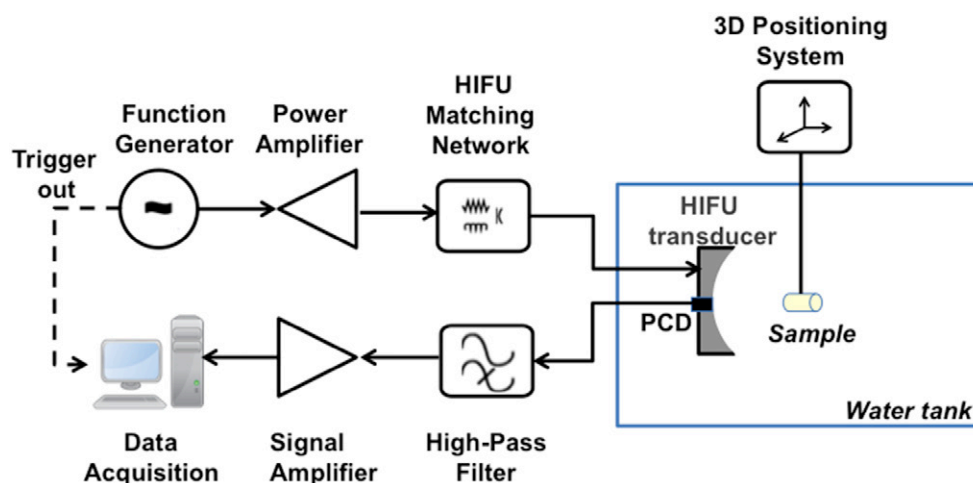
Figure 1. Schematic of the experimental setup. The HIFU transducer was driven by a signal originating from a function generator and amplified by a power amplifier. A matching network was used to optimize power transmission to the HIFU transducer. A passive cavitation detector (confocally aligned with the HIFU transducer) was used to detect cavitation at the focus of the HIFU beam. The signal from the PCD was filtered using a 2 MHz high-pass filter, amplified and then recorded using a data acquisition system for further analysis.

of the holder were 10 mm diameter, and 30 mm length, 4 mm of which was occupied by the donor layer, and 26 mm by the acceptor layer. The axis of the cylinder was aligned with the HIFU axis.

The acceptor layer—prepared by dissolving 3% w/v agar (UltraPure Agarose 1000, Invitrogen, Paisley, UK) in distilled, deionized water and heated until all of the agar powder had dissolved. The liquid solution was then degassed at a pressure of −0.5 bar for 45 min at a temperature of 70 °C and then immediately dispensed using a pipette into a Perspex holder described earlier (Bhatnagar *et al* 2014). Agar at this concentration has speed of sound and density that are close to human tissue (Condliffe 2009).

To prepare the donor layer, the agar powder was mixed at a 0.5% w/v concentration with 0.9% w/v PBS solution (Dulbecco's PBS 1%, Life Technologies, Paisley, UK) and was heated until the agar powder fully dissolved. After degassing and cooling the gel to a temperature of 40 °C, the fluorescently-stained insulin solution described earlier was added to the solution, so that the end insulin concentration of the donor layer was $100\,\mu g\,ml^{-1}$. $300\,\mu l$ of donor solution was used for each sample, so that $30\,\mu g$ of insulin or 0.864 IU were contained in each donor layer. Although this is on the lower end of the scale of insulin doses normally delivered to a diabetes patient, this concentration was the highest that could avoid fluorescent imaging saturation. Samples were placed in a 4 °C fridge between the casting of the donor and acceptor layers for 2 h, and after the casting of the acceptor layer for 1 h to aid the agar gelling process.

Artificial cavitation nuclei have been previously shown to lower the inertial cavitation threshold and to increase the cavitation activity in ultrasound-exposed media (Gyöngy 2010). Such artificial nuclei can take the form of ultrasound contrast agent microbubbles (Arvantis *et al* 2011), or solid gas-entrapping microparticles such as talcum powder (Rifai *et al* 2010). At the combination of pressure and frequency chosen (0.256 MHz, 0.6–1.4 MPa), ultrasound contrast agent microbubbles are almost instantly destroyed (Arvantis *et al* 2011), which would result in varying levels of cavitation activity over the exposure duration. Furthermore, the

buoyancy of microbubbles makes it difficult to ensure an even spatial distribution over the entire surface area of the sample. By contrast, talc microparticles provide a stable supply of cavitation nuclei that enables cavitation activity to be maintained throughout the ultrasound exposure (Bhatnagar *et al* 2014). Based on this observation, talcum powder (86255, particle size >44 μm, Sigma-Aldrich, UK) at a concentration of 0.05% w/v was added to the donor layer before solidification of the agar to half of the agar samples. These samples were used to investigate the effect of cavitation in insulin transport enhancement.

2.4. Sample preparation—porcine skin

Porcine skin was chosen as a human skin model based on the following considerations (Coussios and Roy 2008): the thickness of different layers are similar to the human skin; the elastic properties and cellular composition are comparable; the speed of sound—around $1720 \, \mathrm{m \, s^{-1}}$—is not significantly higher than in human skin, which varies between 1498 and $1650 \, \mathrm{m \, s^{-1}}$. Experiments were performed using full thickness porcine skin. The skin was harvested from the medial thigh of female Landrace pigs, weighing 40–50 kg immediately after sacrifice. Samples were shaved and the fat was removed and cut into 40 × 40 mm pieces and stored in a −20 °C freezer up to a week. Just prior to an experiment skin was thawed at room temperature and then mounted in a Perspex holder. Figure 2 shows photographs of the custom-made Perspex holder used to house the porcine skin samples. From the direction of the HIFU transducer, the holder contains the following layers: a golden-colored, donor layer containing agar and insulin acting as the insulin carrier; porcine skin; transparent, degassed, isotonic saline to provide humidity for porcine skin; and a blue polyurethane ultrasound absorber to avoid reflections of the HIFU beam. Saline was used at room temperature, however heating it to body temperature can result in a lower cavitation threshold. The donor layer was prepared in the same manner as in the section 2.3, with the exception that the diameter was 8 mm and the thickness was 6 mm. Cavitation nuclei were not used in this part of the study.

2.5. Ultrasound exposure

A 265 kHz, single-element HIFU transducer (H117D, S/N –001, Sonic Concepts, USA) was used for sonication. The transducer had a 64 mm aperture and 63 mm focal length, and contained a 16 mm diameter hole in the center to accommodate the co-axial placement of a passive cavitation detector (PCD). The transducer was driven by an RF power amplifier (1040 L, Electronics and Innovation, Rochester, NY, USA) whose input signal was provided by a function generator (33220A, Agilent, Santa Clara, CA. USA). The amplifier output impedance was matched to the HIFU transducer through a customized matching network

The focus of the transducer was aligned with the surface of the donor layer. Samples were first aligned to the ultrasound focus using the PCD transducer driven with a pulser- receiver (DPR300 Pulser Receiver, Imaginant, Pittsford, NY, USA) to monitor the position of the sample until its surface was at the focus. Once positioned at the focus, the samples were exposed to 100 cycles of 10% duty-cycle ultrasound insonation (10 ms on, 90 ms off), giving a total exposure time of 10 s. These parameters were chosen in order to minimize heating effects. Cavitation is known to be a phenomenon that only occurs above a certain rarefactional pressure threshold (Coussios and Roy 2008), hence all pressures quoted in this article will be referring to the peak rarefactional focal pressure (PRFP). Pressures were determined using a prior calibration of the HIFU transducer by a fellow member of the laboratory, using a calibrated needle hydrophone (Onda placed at the HIFU focus. To ensure a variety of exposures
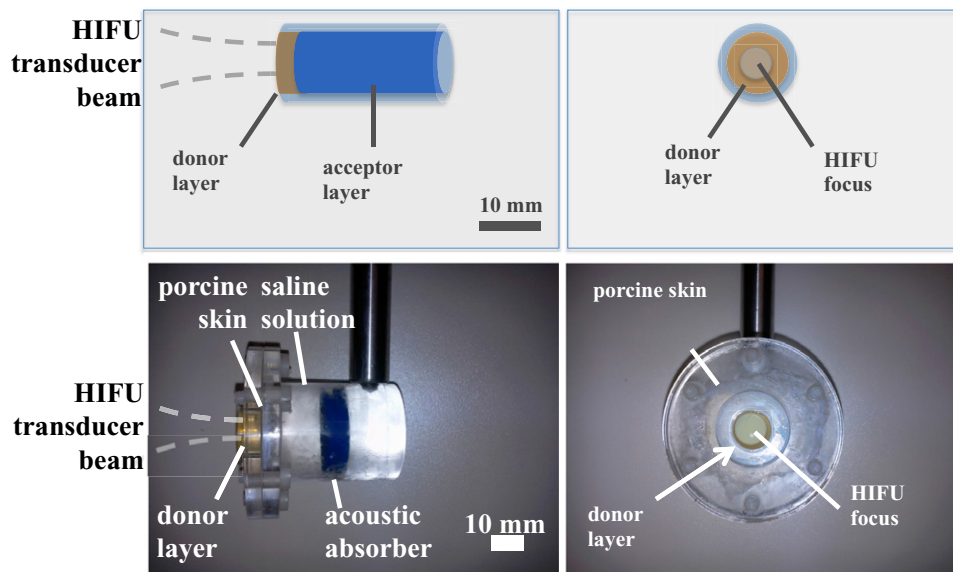
Figure 2. Phantom holders and acoustic alignment of skin models used. The agar skin model (top row) was cylindrical and positioned with the surface of the donor layer at the ultrasound focus. The donor layer in the custom-made Perspex holder for porcine skin (bottom row) was filled with 0.5 w/v% agar hydrogel containing fluorescent insulin at a concentration of $100\,\mu g\,ml^{-1}$. The skin was placed between the donor and acceptor layer using epoxy glue and screws. The acceptor layer was filled with isotonic saline in order to provide osmotic conditions close to that in the body. The HIFU beam was focused at the surface of donor layer.

with and without the occurrence of cavitation, a large range of pressures (0.25, 0.45, 0.65, 1.00, 1.40 MPa) was used in agar. Based on the results in agar, 1.00 and 1.40 MPa was used for porcine skin. Three exposures were carried out for each parameter setting.

2.6. Quantification of inertial cavitation

A 13 mm aperture PCD (V309-SU, PZT element, Olympus Industrial, Southend-On-Sea, UK) detected inertial cavitation by capturing broadband acoustic emissions during ultrasound exposure. It had a central frequency of 5 MHz and a 111% −6 dB bandwidth. The PCD was placed inside a hole running through the central axis of the HIFU transducer (see section 2.5), and the PCD focus was aligned with the HIFU focus to ensure optimal capture of cavitation events.

To record the cavitation, the signal received by the PCD was first filtered with a 2 MHz high-pass filter (Allen Avionics, USA) in order to remove the harmonics of the 265 kHz insonation frequency. The filtered signal was then amplified 25 times using two passes of a 4-channel, 0–350 MHz response, 5 × preamplifier (SR445A, Stanford Research Systems, Sunnyvale, California) and digitized using a 14 bit data acquisition (DAQ) card (PCI-5122, National Instruments, Austin, Texas) operating at a sampling frequency of 100 MHz. The DAQ card was set to record synchronously with the HIFU pulses using an output trigger from the function generator, recording a $200\,\mu s$ segment for each pulse.

To quantify the level of inertial cavitation, digital filtering was applied to remove the harmonics and sub-harmonics of the signal and leave a voltage signal V containing only the

broadband component. The variance of *V* was calculated for each $200\,\mu$s segment and then integrated over time to produce a so-called cavitation dose measure, with units of V^2s that are proportional to energy (Hockham *et al* 2010).

2.7. Quantification of insulin delivery

For quantification of insulin delivery in agar, the agar samples were removed from their Perspex moulds and a 2 mm thick slice was cut out along the plane of the HIFU axis (and thus HIFU focus) using a pair of blades. After removal of the donor layer to avoid image saturation, each slice was mounted on a microscopic slide and analyzed under a fluorescent microscope (Nikon Eclipse Ti, Nikon Instruments, Melville, NY, USA) to determine the insulin concentration and penetration depth in the acceptor layer. Images were taken from each sample under the same exposure settings and ImageJ software (National Institute of Health, Bethesda, Massachusetts) was used to determine the fluorescent intensities.

A fluorescence calibration curve was used to convert the detected fluorescent intensities onto insulin concentrations. The average insulin concentration was calculated in the top 2 mm penetration depth of each of the samples from the average fluorescent intensity present in that area. Penetration distance was defined as the maximum depth from the surface of a sample where fluorescence was above the fluorescence of pure agar.

In the case of porcine samples, each sample was immediately removed from its holder following HIFU exposure and a 3×3 mm piece was cut around the site of the HIFU focus. Samples were quick-frozen using hexane and dry ice to avoid the formation of ice-crystals. Pieces were stored in a $-20\,°$C fridge for up to 2–3 d. Samples were removed from the fridge and stored in dry ice until they were embedded with Tissue–Tek OCT compound (Fisher Scientific, MA, USA) for sectioning with a cryostat. $30\,\mu$m-thick pieces were cut from each of the samples using a cryostat, and then placed onto microscopic slides. Samples were embedded with a mounting medium (Vectashield Mounting Media, Vector Laboratories, California) to help prolonged storage and inhibit photobleaching during fluorescence imaging.

In contrast to the agar samples, the background fluorescence changed with each sample. Therefore, the peak penetration distance was found unreliable. A measure of effective penetration distance (EPD) was defined instead. This measure was calculated as the mean distance value for the normalized (probability) distribution of fluorescent intensities with distance, evaluated over the distance range of 0 to $400\,\mu$m from the skin surface. The average fluorescent intensities were also evaluated over this distance range.

3. Results and discussion

3.1. Results in agar—cavitation dose, transport enhancement

Figure 3 shows the cavitation doses recorded at different pressures. The cavitation threshold is defined as the lowest peak rarefactional pressure amplitude at which the level of broadband emission exceeds twice the noise floor ($0.06\,\mu$J). In the absence of cavitation nuclei, the cavitation threshold is crossed at 1.00 MPa, where the cavitation energy increases to $1.2\,\mu$J. With cavitation nuclei, the threshold is crossed at a pressure as low as 0.65 MPa, where the inertial cavitation energy already reaches $0.2\,\mu$J. At pressures of 0.65 MPa and above, the cavitation dose in the presence of cavitation nuclei slightly exceeds that in the absence of cavitation nuclei. This suggests that cavitation nuclei not only lower the cavitation threshold, but increase the level of cavitation activity and thus potentially the level of transdermal delivery.
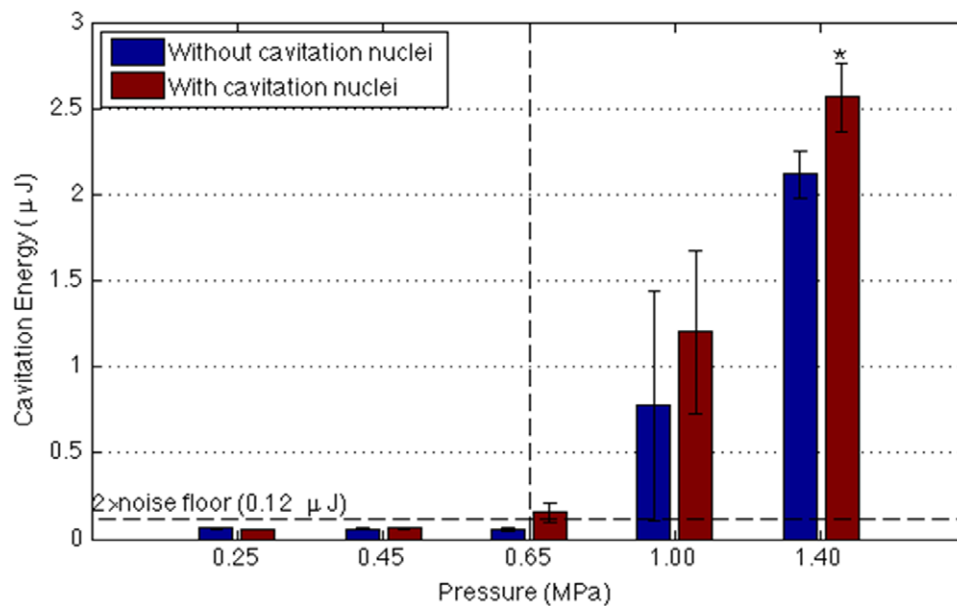
Figure 3. Cavitation dose in agar samples as a function of insonation pressure, with and without cavitation nuclei. The results show that the use of cavitation nuclei lowers the cavitation threshold from between 0.65 and 1 MPa to between 0.45 and 0.65 MPa. The stars denote significant differences compared to the corresponding control group (*: $p < 0.05$, **: $p < 0.01$; two-tailed, unpaired *t*-test).

The structure of the cavitation nuclei allows them to lower the cavitation threshold. Rough surfaced talc particles trap air pockets on the surface, therefore a high peak rarefactional pressure amplitude to draw dissolved gas out of solution is no longer required and the pressure required to cavitate the trapped gas, i.e. the cavitation threshold, is decreased. The results of this study also show that despite the ready supply of bubbles on the surface of cavitation nuclei, their presence does not result in higher levels of broadband emissions detected at the PCD. This is indicated by the lack of significant difference between the groups with and without cavitation nuclei at pressures above the cavitation threshold.

Figure 4 shows the average insulin concentrations in the acceptor layers of agar samples exposed to various ultrasound pressures. In the absence of ultrasound, passive diffusion of insulin raises the average insulin concentration in the acceptor layer to around $5.8\,\mu\mathrm{g}\,\mathrm{ml}^{-1}$. None of the exposures below the cavitation threshold (0.65 MPa with, 1.00 MPa without cavitation nuclei) where inertial cavitation is not present enhance this concentration significantly ($p < 0.05$). For ultrasound exposure at pressures above the cavitation threshold, the concentration is enhanced by over 10% compared to the control. With cavitation nuclei, figure 4 shows that increases in insulin concentration are consistently over 20%, with up to a 40% enhancement observed at 1.4 MPa. The use or omission of cavitation nuclei at a given pressure helps separate purely cavitation-related effects from pressure-related effects contributing towards transdermal delivery (such as acoustic radiation force). The results therefore suggest that the presence of inertial cavitation increases insulin delivery significantly, and that cavitation nuclei increase insulin delivery by increasing the cavitation dose at lower pressures.

Similarly to concentration enhancement, enhancement in peak transport distance is also highly dependent on the presence of cavitation (figure 5). The peak transport distance increases
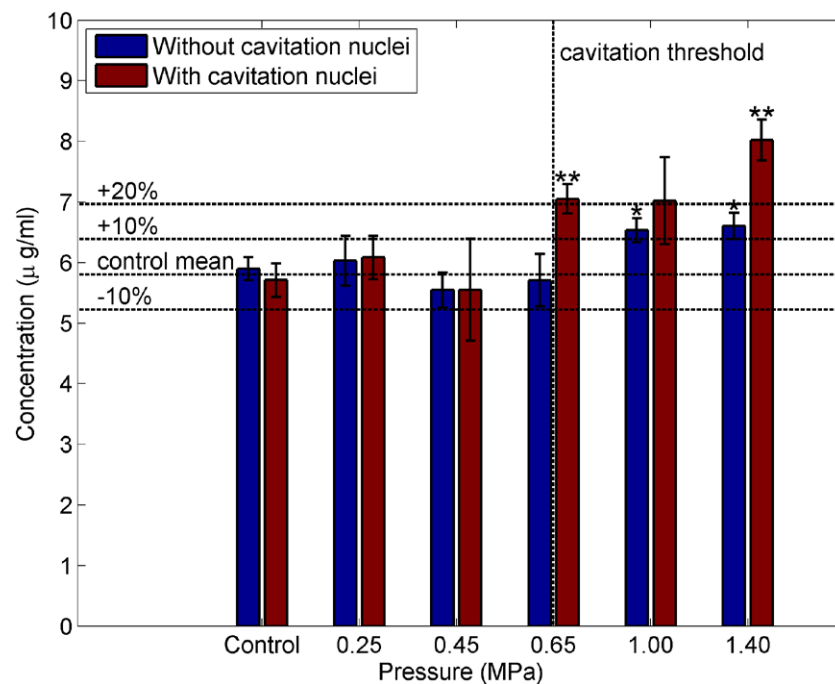
Figure 4. Insulin concentration in the acceptor layer of agar samples as a function of insonation pressure, with and without cavitation nuclei. The stars denote significant differences compared to the corresponding control group (*: $p < 0.05$, **: $p < 0.01$; two-tailed, unpaired *t*-test). There were significant differences at 0.65 MPa with talcum (*p*-value: 0.003), at 1.00 MPa without talcum powder (*p*-value: 0.016), and at 1.40 MPa with talcum powder (*p*-value: 0.0008). There were no significant differences between the results obtained with and without cavitation nuclei. Error bars indicate one standard deviation. The control mean (mean delivered insulin concentration for all control samples) was $5.80 \mu g \, ml^{-1}$. For exposures above the cavitation threshold, the mean insulin concentration is enhanced by at least 10%.

by over 10% above the cavitation threshold. For 3 out of the 5 exposure settings above the cavitation threshold, peak transport distance increased significantly ($p < 0.05$), while none of the sub-threshold exposures exhibited significant enhancement (figure 5). The high variability of cavitation nuclei-associated cavitation is highlighted by the results where they are used. Exposures at 0.45 and 1 MPa show a high variability due to differences in (1) the distribution of cavitation nuclei in individual samples, and (2) the architecture of the individual cavitation nuclei themselves.

Mechanisms for the enhancement in peak insulin penetration distance stem from the presence of inertial cavitation (regardless of the presence or absence of cavitation nuclei) and the resulting formation of microstreams around and adjacent to cavitating bubbles. These microstreams form currents in the agar, carrying the insulin molecules further into the phantom, with the penetration distance of the insulin being proportional to the level of inertial cavitation present.

Although the cavitation threshold is lowered by the addition of cavitation nuclei, no significant change in concentration or penetration depth was found at pressures above the cavitation threshold by the addition of cavitation nuclei. Therefore, in the following experiments in porcine skin, talc powder was not used.
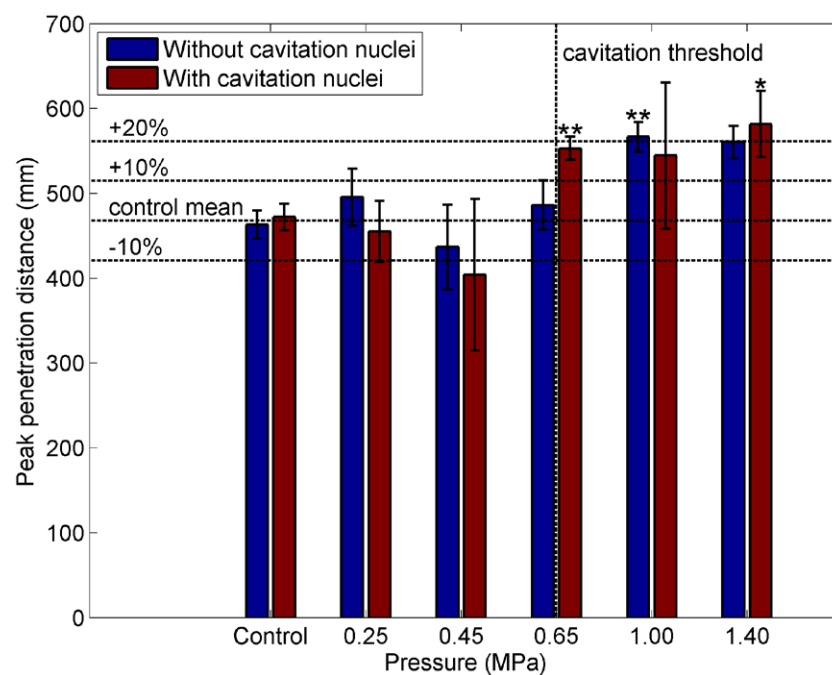
Figure 5. Peak penetration distance in agar samples as a function of insonation pressure, with and without cavitation nuclei. The stars denote significant differences compared to the control (*: $p < 0.05$, **: $p < 0.01$; two-tailed, unpaired *t*-test). There were significant differences at 0.65 MPa with talcum (*p*-value: 0.003), at 1.00 MPa without cavitation nuclei (*p*-value: 0.002), and at 1.40 MPa with cavitation nuclei (*p*-value: 0.027). There were no significant differences between the results obtained with and without cavitation nuclei. Error bars denote one standard deviation. The control mean (mean peak penetration distance for all control samples) was 4.68 mm. For exposures above the cavitation threshold, the peak penetration distance is enhanced by at least 10%. The high variance at 1.00 MPa could be due to a high variance in cavitation energies.

3.2. Results in porcine skin—cavitation activity, transport enhancement

In porcine skin, three insonation pressures were identified that resulted in varying levels of cavitation energy: 0.06 μJ at 0 MPa (control), 0.16 μJ at 1.00 MPa (moderate cavitation dose), and 0.48 μJ at 1.40 MPa (high cavitation dose). As with the agar experiments, each exposure setting was employed three times, and the baseline noise level was 0.06 μJ. Cavitation nuclei were not used in this study, as results in the agar experiments had shown that above the cavitation threshold, the presence of cavitation nuclei did not significantly enhance transport.

Figure 6 shows the fluorescent intensities of three representative porcine samples for the aforementioned three pressures. Unfortunately, the use of tissue made the calibration of absolute insulin concentration difficult, nevertheless, the level of fluorescence intensity is expected to be proportional to the insulin concentration. While insulin uptake is restricted to a few localized regions in control samples, in the presence of inertial cavitation the spatial extent of insulin penetration increased both laterally along the skin surface and in terms of depth, and the delivered concentration is also enhanced.

Another difficulty in comparing insulin delivery in porcine skin samples was that the structure of the skin was inhomogeneous, with differing epidermal thicknesses and the presence of structures such as hair follicles. To minimize the impact of these inhomogeneities,
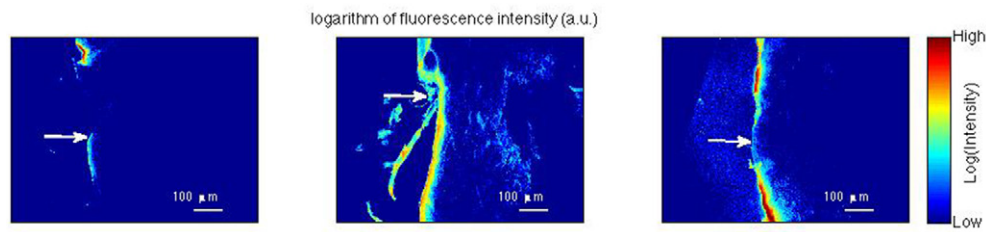
Figure 6. Fluorescence intensity images of insulin distribution in porcine skin following HIFU insonations without ultrasound (left), at 1 MPa (middle) and at 1.4 MPa (right). Insonation was performed horizontally across the images (white arrows), with the depth penetration dimension in the *x*-axis of the image. The fluorescence intensities have been obtained from the green channel of the fluorescence microscope images and have been logarithm compressed to aid interpretation.
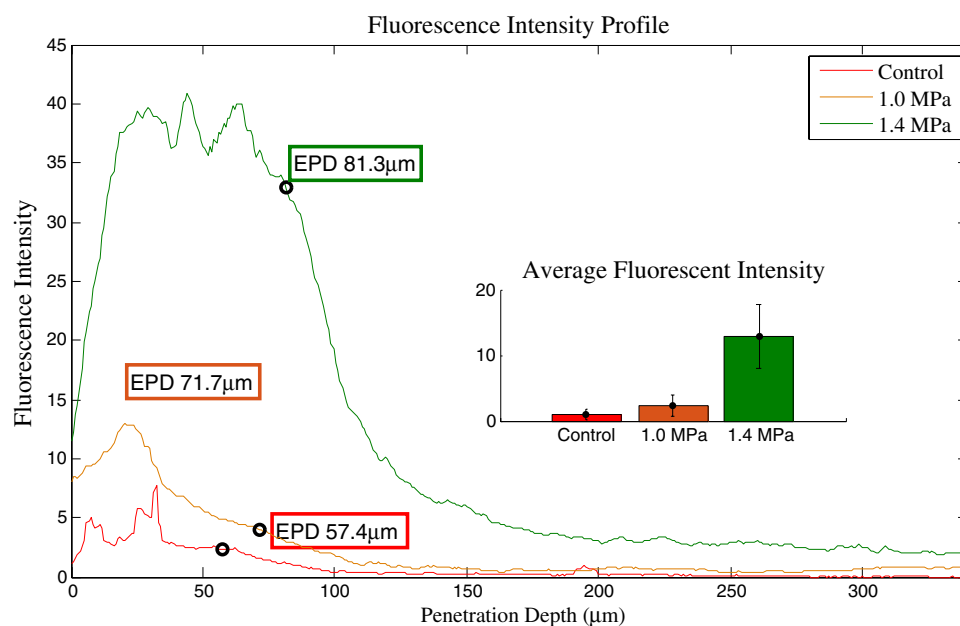

Figure 7. Fluorescent intensity profile of fluorescent insulin as a function of the penetration depth, and average fluorescence intensity (inset) for three pressures. For each pressure, the values were calculated as the average of values obtained from three samples. The recorded cavitation energy for the three pressures was 0, 0.16 and 0.48 μJ respectively. In addition to a modest increase in penetration distance, the significant increase of average fluorescent intensity is thought to be mainly due to the increased cavitation energy present.

regions of interest used for analysis were chosen where the skin structure was similar across samples. Figure 7 shows average fluorescence intensities as a function of depth from the skin surface over three linear profiles in the selected regions of interest, at each exposure condition. As can be seen from the figure, the average fluorescence intensities are significantly higher (at some depths, over 10 times higher) than in the control. The effective penetration distances (marked by red circles on the curves) increased with increasing levels of cavitation energy dose, from 57.4 microns at 0 MPa (in the absence of cavitation)

to 81.3 microns at 1.40 MPa (cavitation energy dose: 0.48 µJ), representing a 40% increase in penetration distance. Even more significant is the more than tenfold increase in average fluorescence intensity compared to control, and a fivefold increase compared to 1.00 MPa. Since the acoustic intensity at 1.40 MPa is less than double than that at 1.00 MPa, this dramatic increase is expected to be primarily due to cavitation, as opposed to other effects such as acoustic radiation force.

4. Conclusions

In the current work, fluorescently-stained, sonophoresis-mediated insulin transport was instigated in two models, 3% agar hydrogel and porcine skin.

In agar, no enhancement in insulin delivery was observed over control (no ultrasound) unless broadband acoustic emissions, attributable to inertial cavitation, were detected by the PCD transducer. Introducing artificial cavitation nuclei in the agar gel lowered the cavitation threshold from 1 to 0.65 MPa, enabling direct comparison of cavitation-mediated and non-cavitation-mediated delivery at the same pressure (0.65 MPa) without affecting other delivery mechanisms such as acoustic radiation force. In the absence of cavitation nuclei there was no enhancement of delivery over control at 0.65 MPa, but in the presence of nuclei, a 20% increase in penetration distance and concentration delivered were observed. At higher pressures above the cavitation threshold (<1 MPa), comparable levels of cavitation activity occur both in the absence and in the presence of cavitation nuclei, and the enhancement in insulin concentration reaches 40% whilst the enhancement in penetration distance reaches 23%. Collectively, these results suggest that the enhancement in delivery is dominated by the level of cavitation activity as detected by the PCD transducer, rather than by the pressure amplitude used or by the presence or absence of artificial cavitation nuclei.

For this reason, no artificial nuclei were used to deliver insulin to skin, instead investigating two pressure amplitudes (1 and 1.4 MPa) that yielded PCD cavitation energies that differed by a factor of 3 (0.16 versus 0.48 µJ). Similarly to the agar results, the occurrence of inertial cavitation caused a modest increase in effective penetration distance of up to 40%. The lower pressure (1 MPa) and cavitation energy resulted in a 2-fold increase in mean delivered fluorescent insulin over control, whilst the higher pressure (1.4 MPa) and cavitation energy yielded a tenfold increase over control. The results indicate a strong correlation between the level of broadband acoustic emissions as detected by a PCD and the observed enhancement in insulin concentration, suggesting that inertial cavitation plays a key role in enhancing transdermal insulin delivery by ultrasound.

Acknowledgments

References

Al-Bataineh O M, Lweesy K and Fraiwan L 2011 *In-vivo* evaluation of a noninvasive transdermal insulin delivery system utilizing ultrasound transducers *J. Med. Imaging Health Inform.* **1** 267–70

Andrews S N, Jeong E and Prausnitz M R 2013 Transdermal delivery of molecules is limited by full epidermis, not just stratum corneum *Pharm. Res.* **30** 1099–109

Arvantis C D, Bazan-Peregrio M and Rifai B 2011 Cavitation-enhanced extravasation for drug delivery *Ultrasound Med. Biol.* **37** 1838–52

Bhatnagar S, Schiffter H A and Coussios C C 2014 Exploitation of acoustic cavitation-induced microstreaming to enhance molecular transport *J. Pharm. Sci.* **103** 1903–12

Boucaud A, Tessier L and Machet L 2000 Transdermal delivery of insulin using low frequency ultrasound *IEEE Ultrasonics Symp.* (*San Juan, October 2000*) **2** 1053–6

Chen W, Brayman A A, Matula T J, Crum L A and Miller M W 2003 The pulse length-dependence of inertial cavitation dose and hemolysis *Ultrasound Med. Biol.* **29** 739–48

Condliffe J 2009 Particle characterization by acoustic microscopy following needle-free injections *Doctoral Thesis*, University of Oxford

Coussios C C and Roy R A 2008 Applications of acoustics and cavitation to noninvasive therapy and drug delivery *Annu. Rev. Fluid Mech.* **40** 395–420

Frenkel V 2008 Ultrasound mediated delivery of drugs and genes to solid tumors *Adv. Drug Deliv. Rev.* **60** 1193–208

Gyöngy M 2010 Passive cavitation mapping for monitoring ultrasound therapy *Doctoral Thesis*, University of Oxford

Händel H, Weise A, Sun W, Pfützer J W, Thomé N and Pfützner A 2008 Difference in the dose accuracy of insulin pens *J. Diabetes Sci. Technol.* **2** 478–81

Hockham N, Coussios C C and Arora M 2010 A real-time controller for sustaining thermally relevant acoustic cavitation during ultrasound therapy *IEEE Trans. Ultrason. Ferroelectr. Freq. Control* **57** 2685–94

Kalluri H and Banga A K 2011 Transdermal delivery of proteins *Am. Assoc. Pharm. Sci.* **12** 431–41

Khafagy E, Morishita M, Onuki Y and Takayama K 2007 Current challenges in non-invasive insulin delivery systems: a comparative review *Adv. Drug Deliv. Rev.* **59** 1521–46

Lai C Y, Fite B Z and Ferrara K W 2013 Ultrasonic enhancement of drug penetration in solid tumors *Front. Oncol.* **3** 204

Levy D and Kost J 1989 Effect of ultrasound in transdermal drug delivery to rats and guinea pigs *J. Clin. Invest.* **86** 2074–8

Mitragotri S, Blankschtein D and Langer R 1995 Ultrasound-mediated transdermal protein delivery *Science* **269** 850–3

Mitragotri S, Blankschtein D and Langer R 1996 Transdermal drug delivery using low-frequency sonophoresis *Pharm. Res.* **13** 411–20

Mitragotri S, Edwards D A, Blanksched D and Langer R 1995 A mechanistic study of ultrasonically-enhanced transdermal drug delivery *J. Pharm. Sci.* **84** 697–706

Mitragotri S, Farell J, Tang H, Terahara T, Kost J and Langer R 2000 Determination of threshold energy dose for ultrasound-induced transdermal drug transport *J. Control. Release* **63** 41–52

Mo S, Coussios C C, Seymour L and Carlisle R 2012 Ultrasound-enhanced drug delivery for cancer *Expert Opin. Drug Deliv.* **9** 1525–38

Ogura M, Paliwal S and Mitragotri S 2008 Low-frequency sonophoresis: current status and future prospects *Adv. Drug Deliv. Rev.* **60** 1218–23

Pearson T L 2010 Practical aspects of insulin pen devices *J. Diabetes Sci. Technol.* **4** 522–31

Pitt W G, Husseini G A and Staples B J 2004 Ultrasonic drug delivery—a general review *Expert Opin. Drug Deliv.* **1** 37–56

Polat B E, Figuera P L, Blankschtein D and Langer R 2011 Transport pathways and enhancement mechanisms within localized and non-localized transport regions in skin treated with low-frequency sonophoresis and sodium lauryl sulfate *J. Pharm. Sci.* **100** 512–29

Polat B E, Hart D and Langer R 2011 Ultrasound-mediated transdermal drug delivery: machanisms, scope, and emerging trends *J. Control. Release* **152** 330–48

Prausnitz M R, Mitragotri S and Langer R 2004 Current status and future potential of transdermal drug delivery *Nat. Rev.* **3** 115–24

Rifai B, Arvantis C D, Bazan-Peregrino M and Coussios C C 2010 Cavitation-enhanced delivery of macromolecules into an obstructed vessel *JASA* **128** 310–5

Saroha K, Sharma B and Yadav B 2011 Sonophoresis: an advanced tool in transdermal drug delivery system *Int. J. Curr. Pharm. Res.* **3** 89–97

Smith N B, Lee S, Maione E, Roy R B, McElligott S and Shung K K 2003 Ultrasound-mediated transdermal transport of insulin *in vitro* through human skin using novel transducer design *Ultrasound Med. Biol.* **29** 311–17

Tang H, Wang C C J, Blankschtein D and Langer R 2002 An investigation of the role of cavitation in low-frequency ultrasound-mediated transdermal drug transport *J. Pharm. Res.* **19** 1060–9

Terahara T, Mitragotri S, Kost J and Langer R 2002 Dependence of low-frequency sonophoresis on ultrasound parameters; distance of the horn and intensity *Int. J. Pharm.* **235** 35–42

Tezel A, Sens A, Tuchscherer J and Mitragotri S 2001 Frequency dependence of sonophoresis *Pharm. Res.* **18** 1694–700

Ueda H, Mutoh M, Seki T, Kobayashi D and Morimoto Y 2009 Acoustic cavitation as an enhancing mechanism of low-frequency sonophoresis for transdermal drug delivery *Biol. Pharm. Bull.* **32** 916–20